

# Catalytic Mechanism of *Escherichia coli* Isopentenyl Diphosphate Isomerase Involves Cys-67, Glu-116, and Tyr-104 as Suggested by Crystal Structures of Complexes with Transition State Analogues and Irreversible Inhibitors\*

Received for publication, December 17, 2002, and in revised form, January 17, 2003  
Published, JBC Papers in Press, January 22, 2003, DOI 10.1074/jbc.M212823200

J. Wouters<sup>‡¶</sup>, Y. Oudjama<sup>‡</sup>, Sam J. Barkley<sup>||</sup>, C. Tricot<sup>‡</sup>, V. Stalon<sup>‡§</sup>, L. Droogmans<sup>§\*\*</sup>,  
and C. Dale Poulter<sup>||</sup>

From the <sup>‡</sup>Institut de Recherches Microbiologiques J.M. Wiame, 1 av E. Gryzon 1070 Bruxelles, Belgium, the <sup>§</sup>Laboratoire de Microbiologie, Université Libre de Bruxelles Campus Ceria, 1 av E. Gryzon 1070 Bruxelles, Belgium, and the <sup>||</sup>Department of Chemistry, University of Utah, Salt Lake City, Utah 84112

**Isopentenyl diphosphate (IPP):dimethylallyl diphosphate (DMAPP) isomerase is a key enzyme in the biosynthesis of isoprenoids. The reaction involves protonation and deprotonation of the isoprenoid unit and proceeds through a carbocationic transition state. Analysis of the crystal structures (2 Å) of complexes of *Escherichia coli* IPP:DMAPPs isomerase with a transition state analogue (*N,N*-dimethyl-2-amino-1-ethyl diphosphate) and a covalently attached irreversible inhibitor (3,4-epoxy-3-methyl-1-butyl diphosphate) indicates that Glu-116, Tyr-104, and Cys-67 are involved in the antarafacial addition/elimination of protons during isomerization. This work provides a new perspective about the mechanism of the reaction.**

Isopentenyl diphosphate (IPP)<sup>1</sup>:dimethylallyl diphosphate (DMAPP) isomerase (EC 5.3.3.2) catalyzes the rearrangement of IPP (Scheme 1, 1) to its electrophilic allylic isomer DMAPP (2). This is a mandatory activation step of the isoprenoid unit for subsequent prenyl transfer reactions in isoprenoid biosynthesis. Isomerization of the carbon-carbon double bond in IPP involves an antarafacial (1, 3) transposition of hydrogen by a proton addition-elimination mechanism (1, 2). During the reaction, a proton is added to the *re*-face of the double bond in IPP, and the *re*-proton at C2 is removed (3).

In eukaryotes, IPP is synthesized by the mevalonate pathway and is the exclusive product from phosphorylation and decarboxylation of mevalonic acid. IPP isomerase activity is an essential enzyme for these organisms. In many bacteria and in

plant chloroplasts, IPP and DMAPP are both synthesized from 4-hydroxydimethylallyl diphosphate by the methylerythritol phosphate pathway (4). Although IPP isomerase is often found in these bacteria, it is not essential. Multiple sequence alignments indicate that *Escherichia coli* IPP isomerase is related to the eukaryotic enzymes (5). In addition, a combination of gas chromatography/mass spectrometry and NMR studies with labeled IPP showed that the stereochemistry for the reversible introduction and removal of a proton at C2 during interconversion of IPP and DMAPP is the same for *E. coli* IPP isomerase and the eukaryotic enzymes (6).

Several lines of evidence support the protonation/deprotonation mechanism shown in Scheme 1. These include proton exchange measurements (7), decreased reactivity for a fluorinated analogue of DMAPP, potent noncovalent inhibition by ammonium analogues of the putative carbocationic intermediate (8, 9), and irreversible inhibition by mechanism-based inhibitors containing epoxide moieties (9–11). Based on the antarafacial stereochemistry for protonation/deprotonation, it has been proposed that IPP isomerase has two active-site bases located on opposite faces of the allylic moiety defined by C2-C3-C4 in IPP. One of these bases is in the conjugate acid form and protonates the double bond. The other assists with the subsequent elimination of a proton (9). Reardon and Abeles (8) presented evidence for involvement of a thiol group during catalysis. The thiol group at Cys-139 was later identified as a catalytic-site residue in yeast IPP isomerase by covalent modification using epoxide (11) and allylic fluoride (12) analogues of IPP. This residue corresponds to Cys-67 in *E. coli* IPP isomerase. Replacement of Cys-139 with serine by site-directed mutagenesis gave a catalytically compromised protein that was covalently modified at Glu-207 upon incubation with 3-(fluoromethyl)-3-butenyl diphosphate (13). Kinetic studies showed that an E207Q yeast mutant was also catalytically compromised (13). This residue corresponds to Glu-116 in *E. coli* IPP isomerase.

The three-dimensional structure of *E. coli* IPP isomerase was recently solved. Crystal structures of free and metal-bound IPP isomerase show that the protein requires a divalent cation to fold into its active conformation (14, 15). Three histidines and two glutamates form a distorted octahedral metal coordination site for the divalent cation. In the structure of *E. coli* IPP isomerase, residues Cys-67 and Glu-116 (corresponding to Cys 139 and Glu-207 in the *Saccharomyces cerevisiae* enzyme) face each other within the active site and are located close to the metal-binding site. Based on this structure, a mechanism was proposed where the cysteine initiates the reaction by protonat-

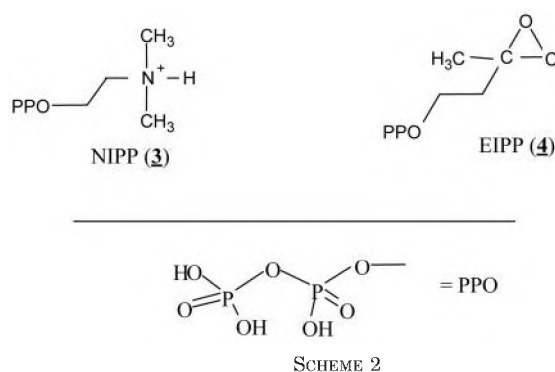
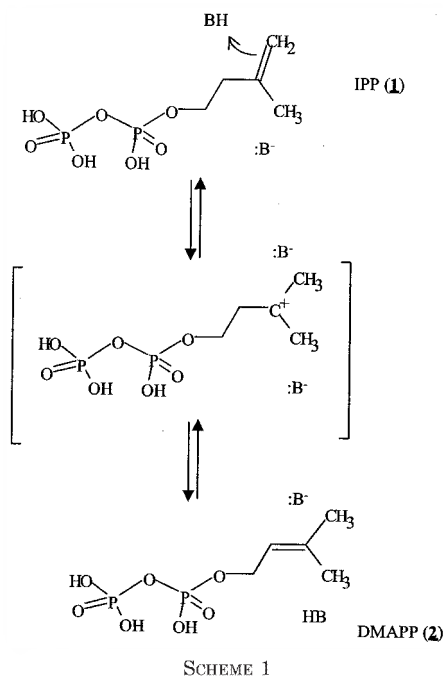
\* This work was supported in part by the Belgian Fonds National de la Recherche Scientifique (FRFC Grant n°2.4529.01), by an 'Action de Recherche Concertée' (ARC) financed by the French Community of Belgium and the Belgian Fund for Joint Basic Research, and by National Institutes of Health Grant GM25521. The costs of publication of this article were defrayed in part by the payment of page charges. This article must therefore be hereby marked "advertisement" in accordance with 18 U.S.C. Section 1734 solely to indicate this fact.

The atomic coordinates and structure factors (code 1NFS and 1NFZ) have been deposited in the Protein Data Bank, Research Collaboratory for Structural Bioinformatics, Rutgers University, New Brunswick, NJ (<http://www.rcsb.org/>).

¶ To whom correspondence should be addressed. Tel.: 32-2-527-36-34; Fax: 32-2-526-72-70; E-mail: [jwouters@dbm.ulb.ac.be](mailto:jwouters@dbm.ulb.ac.be).

\*\* A Research Associate of the Belgian Fonds National de la Recherche Scientifique.

<sup>1</sup> The abbreviations used are: IPP, isopentenyl diphosphate; DMAPP, dimethylallyl diphosphate isomerase; NIPP, *N,N*-dimethyl-2-amino-1-ethyl diphosphate; EIPP, 3,4-epoxy-3-methyl-1-butyl diphosphate.



ing the carbon-carbon double bond and one of the glutamates in the metal coordination sphere (Glu-114 or Glu-116) assists with proton elimination (14).

To gain further insight into the catalytic mechanism of IPP isomerase, we obtained crystal structures of the *E. coli* protein crystallized in the presence of *N,N*-dimethyl-2-amino-1-ethyl diphosphate (Scheme 2, *NIPP*, **3**), a transition state analogue (8, 9), and 3,4-epoxy-3-methyl-1-butyl diphosphate (*EIPP*, **4**), a mechanism-based irreversible inhibitor (9–11). In *NIPP*, the positively charged ammonium group mimics the putative tertiary carbocation formed by protonation of the double bond in IPP. The inhibitor forms a stable noncovalent complex with IPP isomerase.

*EIPP* is an irreversible inhibitor that forms a covalent bond to Cys-139 in the yeast enzyme. Analysis of the crystal structures (1.96 Å) of complexes between those transition state analogues and wild-type *E. coli* IPP isomerase provides evidence for the involvement of Cys-67 and Glu-116 and suggests Tyr-104 may also be part of the catalytic machinery.

#### EXPERIMENTAL PROCEDURES

**IPP Isomerase Activity**—Recombinant *E. coli* IPP isomerase (C-terminal His-tagged) was produced and purified as previously described (16). Prior to enzymatic activity tests or crystallization trials, the protein was treated by EDTA (5 mM) and dialyzed against metal-free 50 mM Tris/HCl (pH 7.4) buffer.

The assay of *E. coli* IPP isomerase is based on the acidic lability of the DMAPP described by Satterwhite (17). The allylic product is hydrolyzed in aqueous acid, whereas IPP is stable. The reaction was initiated by adding the enzyme to the assay mixture constituted of Tris/HCl buffer 50 mM, pH 7.5, and 18 μM [1-<sup>14</sup>C]IPP in a final volume of 50 μl. The effect of divalent cations was tested by addition of Mn<sup>2+</sup> and/or Mg<sup>2+</sup> to the buffer. After incubation at 37 °C, the reaction was stopped by adding 400 μl of methanol/concentrated HCl (4:1, v/v). The mixture was subsequently incubated for 10 min at 37 °C, and the radioactive products were extracted with chloroform. The extraction was facilitated by vigorous vortexing followed by centrifuging at 10,000 × *g* for 2 min. A 200-μl portion of the organic layer was mixed with 5 ml of scintillation mixture (ICN Biomedicals). The radioactivity is counted as a measure for the conversion of IPP into DMAPP.

**Crystallography**—Crystals of *E. coli* IPP isomerase were grown at room temperature by the hanging drop method. Protein (10 mg/ml) was equilibrated against a reservoir containing PEG2000 (16%), ammonium sulfate (100 mM), and MnCl<sub>2</sub> (10 mM) buffered with Tris/maleate at pH 5.5. Complexes were obtained by soaking crystals of the enzyme with

*NIPP* (**3**) and *EIPP* (**4**). Solutions of the inhibitors (25 mM) in Tris/maleate (100 mM, pH 5.5), PEG2000 (16%), ammonium sulfate (100 mM), MnCl<sub>2</sub> (10 mM), and glycerol (25%) were replaced every 8 h for at least 24 h. After soaking, crystals were flash-frozen, and diffraction data were collected with a Mar345 imaging plate system from marresearch equipped with Osmic optics and running on an FR591 rotating anode generator. Diffraction data were processed with the MarFLM suite. In the presence of metal, the protein crystallizes in the space group P2<sub>1</sub>2<sub>1</sub>2, with cell parameters *a* = 69.3, *b* = 72.6, and *c* = 92.5 Å. There are two molecules in the asymmetric unit, related by 2-fold non-crystallographic symmetry. Data sets were recorded at 1.96 Å resolution for the *NIPP* and *EIPP* complexes. Refinements were performed with the program Shelx197 (18) using the structure of unliganded IPP isomerase (Protein Data Bank reference code 1hxz) as starting model. Non-crystallographic restraints were used during the whole refinement (NCSY restrain in Shelx197) except for the conformation of the inhibitor, which was refined independently in the two molecules of the asymmetric unit. As a test, non-crystallographic restraints were removed and further refinement cycles performed. This led to a small drop in *R*<sub>1</sub>, but no significant decrease in *R*<sub>free</sub>. Electron density maps were inspected with the graphical program Turbo-Frodo (19). Quality of the models was analyzed with the program Procheck (20). Final coordinates have been deposited at the Protein Data Bank under codes 1NFS and 1NFZ for the *NIPP* and *EIPP* complexes, respectively.

#### RESULTS

Crystal structures were refined at 1.96 Å resolution for *E. coli* IPP isomerase in complex with *N,N*-dimethyl-2-amino-1-ethyl diphosphate (Scheme 2, *NIPP*, **3**) and 3,4-epoxy-3-methyl-1-butyl diphosphate (*EIPP*, **4**). The quality of the data and the refinement are summarized in Table I. The protein crystallizes with two molecules in the asymmetric unit related by non-crystallographic symmetry. Both molecules adopt an identical fold, and the geometries of the complexes with *NIPP* and *EIPP* are similar.

*E. coli* IPP isomerase folds into a compact globular protein that belongs to the class of α/β proteins, with an original architecture (Fig. 1). In the presence of divalent metal, the N-terminal residues fold into a small β-sheet domain of two antiparallel strands that partly covers a pocket comprising the putative catalytic site. This domain is not observed in the absence of metal (14). In the metal-bound, active conformation, the protein forms a unique distorted octahedral metal coordination site composed of residues His-25, His-32, His-69, Glu-114, and Glu-116 (Fig. 1). Both carboxylate oxygens of Glu-114 coordinate to the metal. In contrast, only one carboxylate oxygen of Glu-116 coordinates with the metal, and the other oxygen faces the thiol group of Cys-67, which is ~7 Å away.

Unambiguous electron density in the initial Fourier difference (*F<sub>o</sub>* - *F<sub>c</sub>*) maps (contoured at 3σ) revealed the location and conformation of the transition state analogue *NIPP* (**3**) and the irreversible inhibitor *EIPP* (**4**) in the structures of the two complexes (Fig. 2). Simulated annealing omit maps of the refined models confirmed the placement on each inhibitor in the active sites.

**Complex with *NIPP***—In the complex of *E. coli* isomerase

TABLE I  
Data collection and refinement statistics

	NIPP	EIPP
Crystal data		
Space group	P2 <sub>1</sub> 2 <sub>1</sub> 2 <sub>1</sub>	P2 <sub>1</sub> 2 <sub>1</sub> 2 <sub>1</sub>
Cell dimensions (Å)	69.105 72.223 91.722	69.101 72.106 91.520
Subunits per asymmetric unit	2	2
Data set		
Wavelength (Å)	1.54179	1.54179
Highest resolution (Å)	1.97	1.97
Total reflections	107068	102886
Unique reflections	27788	28408
Observed reflections ( $I > 2\sigma(I)$ )	23302	26786
Completeness (%) <sup>a</sup>	94.8 (94.8)	98.8 (97.2)
$R_{\text{merge}}$ (%) <sup>a</sup>	4.2 (24.4)	3.7 (10.1)
$I/\sigma(I)$	9.2	8.8
Refinement		
Resolution range (Å)	10–1.97	10–1.97
Number of protein atoms	2822	2822
Number of ligand atoms	32	34
Number of water molecules	117	298
$R_{\text{cryst}}$ (observed/all data) (%)	21.0/22.2	17.6/18.0
$R_{\text{free}}$ (%)	26.2	23.7
Root mean square deviations		
Bond lengths (Å)	0.005	0.006
Bond angles (Å)	0.019	0.021
Average B-factor		
All protein atoms (Å <sup>2</sup> )	35.38	26.95
All ligand atoms (Å <sup>2</sup> )	41.80	36.16
All water molecules (Å <sup>2</sup> )	36.94	34.31
Ramachandran plot <sup>c</sup>		
Most favored regions (%)	89.2	88.2
Additionally allowed region (%)	10.8	11.8
Generously allowed region (%)	0.0	0.0
Disallowed region (%)	0.0	0.0

<sup>a</sup> Statistics for the highest resolution shell (2.08–1.97 Å) are given in parentheses.

<sup>b</sup> Free test subset represents 10% of total unique reflections.

<sup>c</sup> As defined by PROCHECK, Gly and Pro residues excluded.

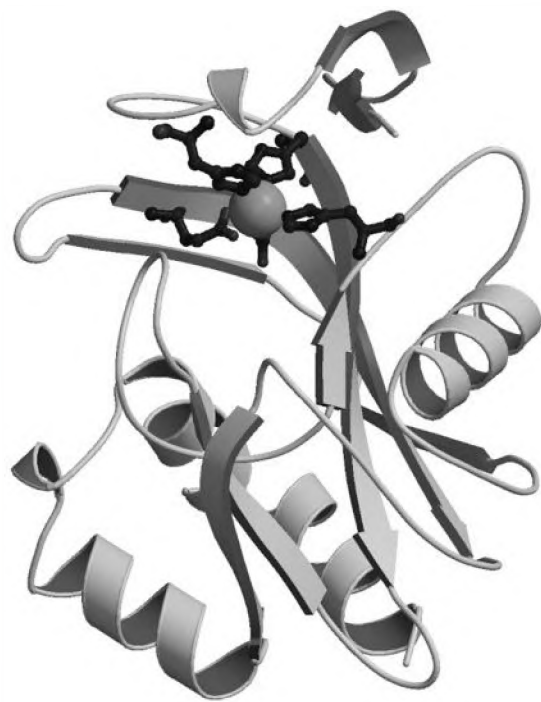


FIG. 1. Overall fold with secondary structure elements and metal binding site.

with NIPP (**3**), the inhibitor adopts an extended conformation with the positively charged ammonium moiety between Glu-116 and Cys-67 (Fig. 3a). Main torsion angles defining the

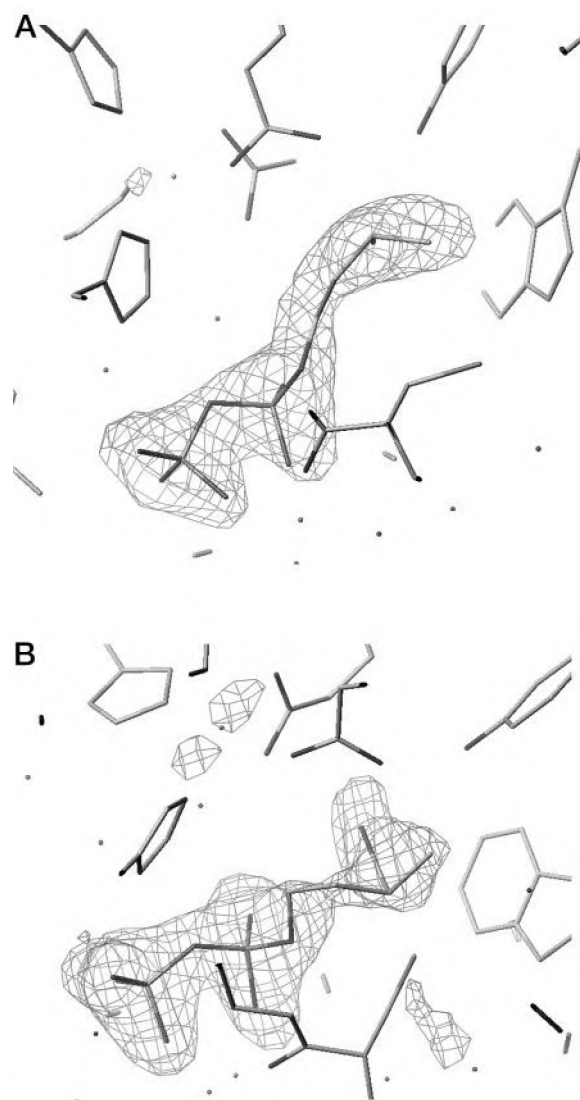


FIG. 2. Difference Fourier density ( $F_o - F_c$ ) map for NIPP (A) and EIPP (B). Density comes from an omit map calculated after the refinement of the protein but prior to placement of the inhibitors. The refined position of the inhibitors is shown.

conformation of NIPP are given in Table II, together with selected interactions with surrounding residues of the active site.

The geometry around nitrogen atom N1 is tetrahedral, as expected. The two methyl groups are displaced toward Cys-67, and the nitrogen atom is protonated. In this geometry, N1 is optimally placed to be stabilized by an ionic interaction involving the oxygen atom of Glu-116 that is not directly coordinated with the divalent metal (N1 (**3**)-OE1 (Glu-116) distance about 2.7 Å, Table II). Proximity of the divalent metal cation binding site should stabilize the carboxylate form of Glu-116.

The hydroxyl group of Tyr-104 is near OE1 of Glu-116. Interestingly, this residue is highly conserved in IPP isomerases. Its location in the active site, H-bonded to Glu-116, suggests that it could be involved in the proton transfer to substrates/inhibitors. However, the precise role that Tyr-104 residue plays during catalysis is not understood.

Trp-161 is also optimally positioned in the active site to interact with the positively charged ammonium moiety in NIPP and presumably stabilizes the developing positive charge at C3 of IPP or DMAPP during isomerization through a  $\pi$ -cation interaction (21, 22). This observation is among the first that provides direct

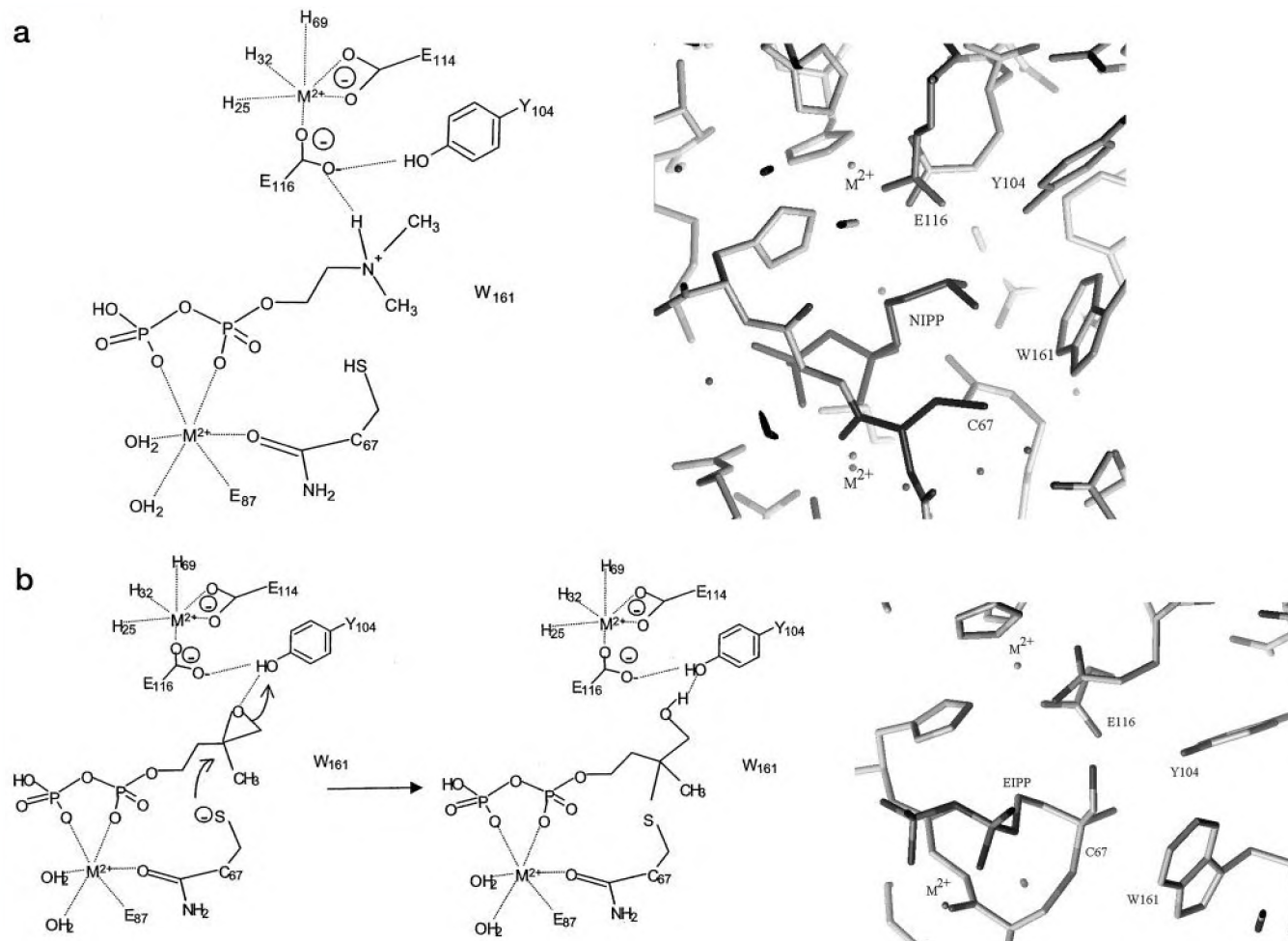


FIG. 3. View of the binding site of wild-type IPP isomerase in complex with NIPP (a) and EIPP (b).

experimental evidence for a  $\pi$ -cation interaction in a protein-transition state analogue complex. A  $\pi$ -cation interaction involving the polarizable indole ring in Trp-161 may explain the reduced activity reported for the W161F mutant (14).

The diphosphate group in NIPP is stabilized by a dense network of ionic and H-bond interactions. A second divalent metal ion interacts with a non-bridging oxygen of each phosphorus to form a six-membered ring chelate whose geometry is similar to that found in crystal structures of other diphosphate binding proteins, including isoprenoid diphosphate cyclases and flavoproteins or dehydrogenases that stabilize the diphosphate moieties of the FAD or NAD(P) cofactors.

The diphosphate group is further stabilized by interactions with Arg-51, Lys-55, Glu-83, and Lys-21 (Table II). The relative importance of those residues has been confirmed by site-directed mutagenesis (14).

Ordered water molecules have also been located in the active site of *E. coli* IPP isomerase. Although not directly involved in the catalysis, they could play a role in stabilization of the substrate/inhibitor in the active site of the protein. No water molecules were located close to the ammonium moiety in NIPP (corresponding to the positively charged center of the putative tertiary carbocationic intermediate). The water molecules in the active site of IPP isomerase participate in a network of H-bonds involving the phosphate-bound divalent metal and Glu-87 and stabilize the diphosphate moiety of NIPP. Interestingly, in the absence of inhibitor, the active site of the reported structure of *E. coli* IPP isomerase (14) contains molecules of imidazole and phosphate from the buffer that lie between Glu-

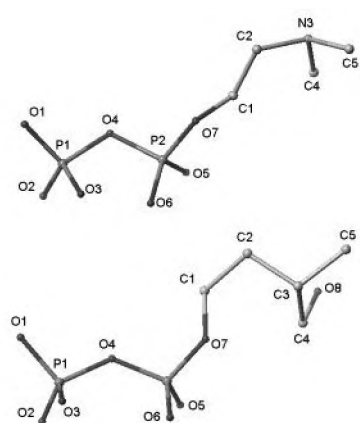
116/Tyr-104 and Cys-67. No water molecules connect those residues. It is, however, anticipated that water molecules would occupy this site in the absence of other ligands (inhibitor, substrate, imidazole).

**Complex with EIPP**—In the complex of *E. coli* isomerase with EIPP, electron density is observed consistent with a covalent bond between the sulfur of Cys-67 in the active site and C3 of the inhibitor (Fig. 3b). Thus, the epoxide in 4 has been opened with concomitant alkylation of thiol moiety in Cys-67. The newly formed hydroxyl moiety at C4 forms a strong H-bond with Tyr-104 with a distance about 2.9 Å (Table II). Although the H atom is not observed, it is reasonable to suggest that the hydroxyl group in Tyr-104 is unprotonated based on the  $pK_a$  differences between phenols and alcohols and serves as H-bond acceptor for the  $O_2$  hydroxyl group in the covalently bound inhibitor. This leads to the hypothesis that the hydroxyl group in Tyr-104 may donate its proton (*via* Glu-116) to the substrate/inhibitor. The conformation of EIPP (Table II) is similar to that seen for enzyme-bound NIPP. Like the NIPP complex, the diphosphate moiety of EIPP is stabilized by interactions with a divalent metal ion and residues Arg-51, Lys-55, Glu-83, and Lys-21 (Table II).

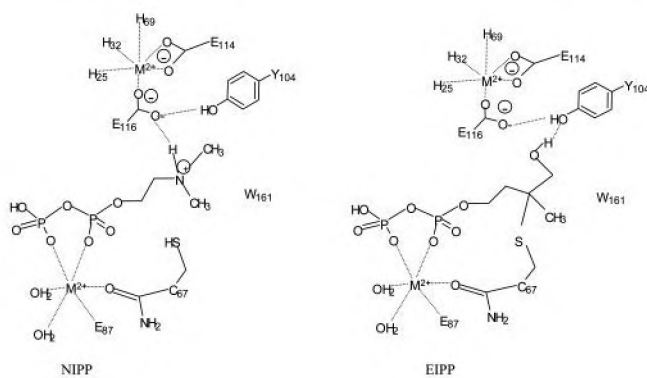
#### DISCUSSION

Extensive kinetic characterization of NIPP with IPP isomerase from *Claviceps purpurea* showed that NIPP formed a stable non-covalent complex with the enzyme with a dissociation constant  $K_D < 1.2 \times 10^{-10}$  M (9). The enzyme-inhibitor complex was stable in 6 M urea, but the inhibitor was partially released

TABLE II  
Selected geometric features for complexes of IPP isomerase with NIPP  
(top) and EIPP (bottom)



Dihedral (°)	NIPP A	NIPP B	EIPP A	EIPP B
O1-P1-O4-P2	167.8	-83.3	-64.9	-75.1
P1-O4-P2-O7	-125.9	-141.5	-144.0	-129.4
O4-P2-O7-C1	-102.5	-27.1	-53.3	-60.0
P2-O7-C1-C2	168.9	163.7	-177.4	-112.4
O7-C1-C2-X <sup>a</sup> 3	156.2	90.4	41.1	55.3
C1-C2-X3-C4	-114.8	-133.9	43.8	24.5



Distance (Å)	NIPP A	NIPP B	EIPP A	EIPP B
O1 - NZ_Lys 55	2.86	2.80	2.77	2.77
O2 - NH2_Arg 83	2.55	3.34	2.95	2.73
O3 - NZ_Lys 21	2.91	2.96	2.90	2.98
O5 - NH2_Arg 51	2.94	2.76	2.82	2.64
N12 - OE1_Glu 116	2.72	2.69		
O8 - OH_Tyr 104			2.37	3.39
M <sup>b</sup> - NE2_His 25	2.09	2.02	2.05	2.05
M - NE2_His 32	2.05	1.97	2.12	2.03
M - NE2_His 69	1.97	2.06	2.16	2.09
M - OE1_Glu 114	2.49	2.39	2.23	2.37
M - OE2_Glu 114	2.07	2.15	2.99	2.18
M - OE1_Glu 116	1.86	1.98	2.05	2.11
M <sup>b</sup> - O2	1.92	2.33	2.01	2.04
M - O6	1.79	1.71	1.99	1.88
M - O_Cys 67	2.09	2.49	2.11	2.23
M - OE1_Glu 87	2.02	1.91	2.22	2.11
M - HOH	2.06	2.09	2.07	2.20
M - HOH	1.92	1.98	1.93	2.18

<sup>a</sup> X = N (NIPP) or C (EIPP).

<sup>b</sup> Two distinct divalent metal cations are located in the binding site of IPP isomerase, one associated to His-25, His-32, His-69, Glu-114, Glu-116 and the other binding to Cys-67, Glu-87 and the diphosphate group of the inhibitors.

upon treatment with SDS and 2-mercaptoethanol at 37 °C for 1 h. The results indicate that NIPP is a transition state/reactive intermediate analogue where the positively charged ammonium group mimics a putative tertiary carbocation formed upon protonation of the carbon-carbon double bonds in IPP or

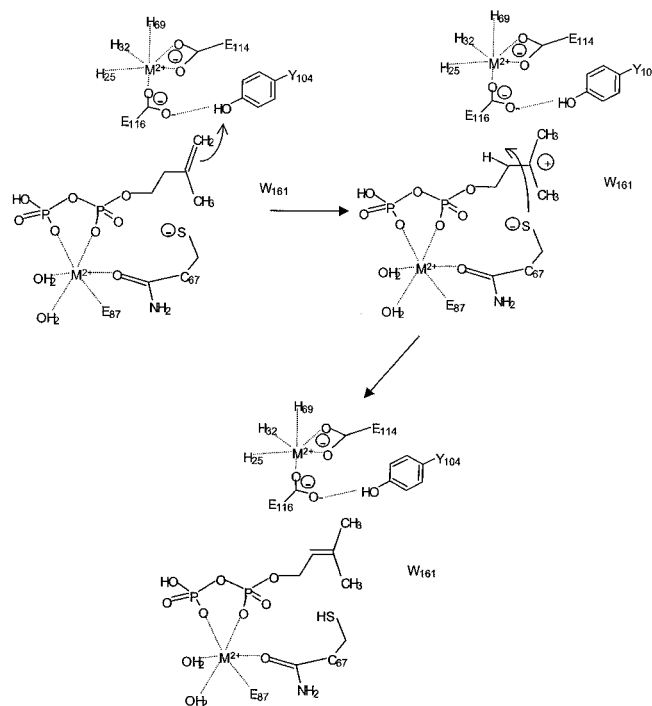


FIG. 4. Proposed mechanism for isomerization of IPP to DMAPP based on the structures of complexes with NIPP and EIPP. Evidence from the crystal structures of complexes with NIPP and EIPP strongly points to Tyr-104 being the proton donor. Glu-116 is likely the critical acidic residue that drives protonation by lowering the energy of the carbocation.

DMAPP during catalysis. In contrast, EIPP is an irreversible inactivator of the yeast and *E. coli* proteins. The epoxide forms a stable covalent adduct that is stable to ion-exchange chromatography and gel electrophoresis (9).

The crystal structures of *E. coli* IPP isomerase complexed with NIPP and EIPP support a mechanism for isomerization in which the first step is the protonation of the unactivated carbon-carbon double bond in IPP or DMAPP. The orientation of NIPP in the complex shows that metal-chelated Glu-116 is optimally positioned to interact with substrate (Fig. 2). Protonated enzyme-bound NIPP is stabilized, in part, by an ionic interaction with unprotonated Glu-116. Additional stabilization is provided by a cation- $\pi$  interaction with the indole side chain of Trp-121. A similar stabilization is expected for the tertiary carbocationic species formed during the enzyme-catalyzed isomerization.

The origin of the protonating H has not been conclusively established. Glu-116 is an essential active-site residue. It is directly ligated to the divalent metal, which will stabilize the carboxylate form of the side chain carboxylic acid. Even in the absence of inhibitor/substrate, Glu-116 is probably unprotonated, given the location of Glu-116 in the inner coordination sphere of the metal. However, the structure of the complex with NIPP strongly suggests that protonation of substrate involves Glu-116 and that the metal-stabilized carboxylate moiety stabilizes the carbocationic intermediate. No ordered water molecules that could serve as proton donors during catalysis are observed near Glu-116. However, Tyr-104 is H-bonded to the side chain carboxylate in Glu-116, both in the unliganded structure of IPP isomerase (14) and in the NIPP complex. The phenolic hydroxyl group in Tyr-104 might be the source of the proton transferred to the double bond in IPP *via* Glu-116.

In the presence of EIPP, Cys-67 acts as a nucleophile that opens the epoxide ring and forms a covalent bond to C3 (Fig. 2). Presumably, the initial stage of the inactivation reaction involves protonation of the oxygen, in analogy to the protonation

of the double bond in IPP during catalysis, followed by nucleophilic attack of the activated epoxy by the side chain thiol group in Cys-67. Although not essential, deprotonation of the thiol prior to the nucleophilic displacement would facilitate the reaction. Thus, it is likely that Cys-67 acts as a base to facilitate removal of the proton from carbocationic intermediate during the isomerization.

The interconversion of IPP and DMAPP proceeds by an antarafacial protonation/deprotonation of the molecules. The x-ray structures of NIPP and EIPP complexes with IPP isomerase suggest that the active site of the enzyme has an acid positioned on one side of the hydrocarbon moiety of the substrate and a base on the other. Whether IPP and DMAPP need to bind to the active site in different conformation to account for the antarafacial stereochemistry of the reaction is not fully answered. The residues that donate and abstract protons in isomerization of IPP (probably Tyr-104 and Cys-67, respectively) likely exist as an equilibrium mixture of protonated and unprotonated forms. They thus would be capable of reversing roles for isomerization of DMAPP (that is, the protonated form of Cys-67 would be the proton donor to DMAPP, and Tyr-104 would be the proton acceptor). In both reactions Glu-116 could still act as the essential acid (but not proton source) that helped drive the formation of the carbocation. Determination of the  $pK_a$  of Cys-67 or Tyr-104 in the enzyme would give some idea of how effective they would be as proton donors and acceptors. Although the deprotonation step is highly stereo- and regio-selective, prolonged incubation of IPP and DMAPP in  $D_2O$  results in exchange of all of the hydrogens on carbons adjacent to C3 in the tertiary cationic intermediate (7).

A mechanism for isomerization of IPP to DMAPP, which is consistent with the structural features of the complexes of *E. coli* IPP isomerase with NIPP and EIPP, is presented in Fig. 4. These features are summarized as follows.

1. The diphosphate moiety of the ligand is stabilized by a network of H-bonds and ionic interactions that involves a divalent metal and residues Arg-51, Lys-55, Glu-83, and Lys-21.

2. The reaction is initiated by protonation of the double bond with involvement of Glu-116. The proton could be given directly by this residue or could come from Tyr-104 located within H-bonding distance of the carboxylate group of Glu-116. The

possibility that the proton comes from water cannot be excluded but seems less probable because an appropriately positioned water molecule has not been detected thus far.

3. The tertiary carbocationic intermediate is stabilized by the metal-activated carboxylate form of Glu-116 and by a cation- $\pi$  interaction with the indole side chain of Trp-121.

4. The thiol moiety of Cys-67, presumably in the thiolate form, assists in removing the proton from the tertiary cation. Following catalysis, the thiol proton Cys-67 would then be recycled to Glu-116/Tyr-104.

#### REFERENCES

- Cornforth, J. W., and Popjak, G. (1969) *Methods Enzymol.* **15**, 359–371
- Poulter, C. D., and Rilling, H. C. (1981) in *Biosynthesis of Isoprenoid Compounds*, (Porter, J. W., and Porter, S. L. eds), Vol. 1, pp. 162–209, John Wiley and Sons, New York
- Clifford, K., Cornforth, J. W., Mailaby, R., and Phillips, G. T. (1971) *J. Chem. Soc. Chem. Commun.* 1699–1700
- Hoeffler, J. F., Hemmerlin, A., Grosdemange-Billard, C., Bach, T. J., and Rohmer, M. (2002) *Biochem. J.* **366**, 573–583
- Hahn, F. M., Hurlburt, A. P., and Poulter, C. D. (1999) *J. Bacteriol.* **181**, 4499–4504
- Leyes, A., Baker, J. A., Hahn, F. M., and Poulter, C. D. (1999) *Chem. Commun.* 717–718
- Street, I. P., Christensen, D. J., and Poulter, C. D. (1990) *J. Am. Chem. Soc.* **112**, 8577–8578
- Reardon, J. E., and Abeles, R. H. (1986) *Biochemistry* **25**, 5609–5616
- Muelherbacher, M., and Poulter, C. D. (1988) *Biochemistry* **27**, 7315–7328
- Poulter, C. D., Muelherbacher, M., and Davis, D. R. (1989) *J. Am. Chem. Soc.* **111**, 3740–3742
- Lu, X. J., Christensen, D. J., and Poulter, C. D. (1992) *Biochemistry* **31**, 9955–9960
- Street, I. P., and Poulter, C. D. (1990) *Biochemistry* **29**, 7531–7538
- Street, I. P., Coffman, H. R., Baker, J. A., and Poulter, C. D. (1994) *Biochemistry* **33**, 4212–4217
- Durbecq, V., Sainz, G., Oudjama, Y., Clantin, B., Bompard-Gilles, C., Tricot, C., Caillet, J., Stalon, V., Droogmans, L., and Villeret, V. (2001) *EMBO J.* **20**, 1530–1537
- Bonanno, J. B., Edo, C., Eswar, N., Pieper, U., Romanowski, M. J., Ilyin, V., Gerchman, S. E., Kycia, H., Studier, F. W., Sali, A., and Burley, S. K. (2001) *Proc. Natl. Acad. Sci. U. S. A.* **98**, 12896–12901
- Oudjama, Y., Durbecq, V., Sainz, G., Clantin, B., Tricot, C., Stalon, V., Villeret, V., and Droogmans, L. (2001) *Acta Crystallogr. Sect. D Biol. Crystallogr.* **57**, 287–288
- Satterwhite, D. M. (1985) *Methods Enzymol.* **110**, 92–99
- Sheldrick, G. M., and Schneider, T. R. (1997) *Methods Enzymol.* **277**, 319–343
- Roussel, A., and Cambillau, C. (1992) *Turbo-Frodo Biographies, Architecture et Fonction des Macromolécules Biologique*, University of Marseille, France
- Laskowski, R. A., McArthur, M. W., and Thornton, J. M. (1993) *J. Appl. Crystallogr.* **26**, 283–291
- Wouters, J. (1998) *Protein Sci.* **7**, 2472–2475
- Dougherty, D. A. (1996) *Science* **271**, 163–168